

# Statistical properties of backscattered semiconductor laser radiation with different degrees of coherence

A.E. Alekseev, Ya.A. Tezadov, V. T. Potapov

**Abstract.** This paper compares the statistical properties of the backscatter intensity in a single-mode optical fibre for semiconductor lasers with a high and a low degree of coherence. We demonstrate that, when short probe pulses are used, shorter than the coherence times of the lasers, the statistical properties of the backscatter intensity obtained with the two lasers are identical, and the intensity distribution over an ensemble of independent fibre sections has an exponential form for both. With increasing probe pulse duration, the backscatter intensity distribution obtained with the shorter coherence time laser approaches a Gaussian one, whereas the distribution function obtained with the high-coherence laser remains nearly exponential. Reflectograms of a coherent reflectometer that relies on the detection of backscattered radiation have the highest contrast for an exponential backscatter intensity distribution over an ensemble of independent fibre sections. The reflectometer then probably has the highest sensitivity to external influences. This leads us to conclude that, when short probe pulses are used, which ensure high spatial resolution (10 m and better), one can use a laser with a short coherence time, equal to the pulse duration.

**Keywords:** semiconductor laser, optical fibre, backscattered radiation, coherent reflectometer.

## 1. Introduction

In recent years, with the advent of inexpensive distributed-feedback semiconductor lasers for telecommunication systems, there has been increased interest in reflectometers that employ such lasers as coherent light sources [1–6]. The emission bandwidth of such lasers is typically 2–5 MHz, which corresponds to coherence times from 160 to 60 ns. In addition, the advent of highly coherent semiconductor lasers with an emission bandwidth of 10 kHz or even less (coherence time, 30  $\mu$ s) has opened up new possibilities for coherent reflectometry.

The purpose of this work is to compare the statistical properties of the time-averaged backscatter signal from a fibre section for an ensemble of independent sections using a standard telecom semiconductor laser with an emission band-

width of 2 MHz and a highly coherent semiconductor laser with an emission bandwidth of 5 kHz. The theoretical and experimental data obtained are used to identify conditions under which a particular laser ensures high contrast of reflectograms for a coherent reflectometer. To our knowledge, no such analysis has been reported previously.

## 2. Theoretical model

Results of theoretical and experimental studies of the statistics of the backscatter intensity distribution in a single-mode optical fibre in relation to the coherence time of the semiconductor laser were presented elsewhere [7, 8]. Such a scattering medium can be modelled by a long fibre section, of length  $L$ , containing uniformly distributed scattering centres in the form of refractive index microinhomogeneities. Their size is much less than the laser wavelength. The centres scatter incident radiation in all directions. Part of the radiation remains in the fibre and propagates in the reverse direction [9]. The interference of the scattered fields gives the resultant scattered radiation intensity for a given section of the fibre. Considering scattering from different, statistically independent sections of a fibre of length  $L$ , we can find the time-averaged scattering intensity distribution over the ensemble. It is worth pointing out that the instantaneous scattering intensity in each fibre section fluctuates in time about the slowly varying time-averaged intensity envelope [10]. The time-domain statistics of such fluctuations in one fibre section were considered in detail by Gysel and Staubli [11], and the corresponding statistics of the current through the photodetector were analysed in Refs [12, 13]. Here, we do not consider such temporal fluctuations. Intensity is here taken to mean the time-averaged intensity scattered from a fibre section occupied by a pulse. Note that the averaging time, about 5 ms, considerably exceeds the coherence time of the source but is shorter than the characteristic time of variations in the scattered intensity envelope.

The dependence of the time-averaged scattered coherent radiation intensity on the spatial position of a probe pulse (reflectogram) has the form of a noise-like signal, which slowly varies in time when the fibre is not subject to any external influences. If a fibre section is subject to an external influence, the corresponding region of the reflectogram undergoes changes, which can be related to parameters of the external influence. The backscatter intensity distribution over the ensemble of independent fibre sections depends on the relationship between the probe pulse duration (spatial pulse width) and the coherence time of the light source. The smaller the ratio of the coherence time to the probe pulse duration, the less time-correlated are the fields scattered by different centres within the scattering region, and vice versa: as the

A.E. Alekseev, Ya.A. Tezadov IRE-Polus Science and Technology Association, pl. Vvedenskogo 1, 141190 Fryazino, Moscow region, Russia; e-mail: aleksey.e.alekseev@gmail.com;

V. T. Potapov V.A. Kotel'nikov Institute of Radio Engineering and Electronics (Fryazino Branch), Russian Academy of Sciences, pl. Vvedenskogo 1, 141190 Fryazino, Moscow region, Russia

Received 4 August 2011; revision received 1 November 2011  
*Kvantovaya Elektronika* 42 (1) 76–81 (2012)  
Translated by O.M. Tsarev

coherence time increases and approaches the probe pulse duration, the scattered fields become better correlated in time. As a result, when the scattered fields are weakly correlated in the former case, the interference pattern of the scattered radiation will have a smaller modulation depth in comparison with the strong correlation in the latter case [8].

The limiting case of the scattering of completely polarised monochromatic radiation can be considered using the random phasor model [14, 15]. In our case, the phasor is the complex amplitude of the radiation scattered by a centre within the scattering region of the fibre. The final result is the scattered intensity distribution over the ensemble of statistically independent fibre sections (intensity distribution function of the reflectogram), which has an exponential form:

$$p_I(I) = \frac{1}{2\sigma^2} \exp\left(-\frac{I}{2\sigma^2}\right). \quad (1)$$

Here,  $I \geq 0$  is the scattered intensity and  $\sigma^2$  is the variance of the distribution, related to the mean absolute squares of all the scattering amplitudes for the scattering centres in the fibre section under consideration. For an exponential distribution, the variance over an ensemble of independent fibre sections is equal to the mean intensity:

$$E\langle I \rangle = \sigma. \quad (2)$$

As the contrast of the resultant reflectogram, we take the ratio of the variance of the intensity distribution to the mean intensity [15]:

$$C = \frac{\sigma}{E\langle I \rangle}; \quad (3)$$

The contrast of an exponential distribution is unity.

Scattering of quasi-monochromatic polarised radiation of a semiconductor laser can be analysed using the Karhunen–Loeve expansion of a random scattered-radiation field in terms of orthonormal functions [8, 14, 15]. The final result is the scattered quasi-monochromatic radiation intensity distribution over the ensemble of statistically independent fibre sections (intensity distribution function of the reflectogram):

$$p_I(I) = \sum_{n=0}^{\infty} \frac{\lambda_n^{-1} \exp(-I/\lambda_n)}{\prod_{\substack{m=0, \\ m \neq n}}^{\infty} (1 - \lambda_m/\lambda_n)} = \sum_{n=0}^{\infty} \frac{d_n}{\lambda_n} \exp\left(-\frac{I}{\lambda_n}\right) \quad (4)$$

for  $I \geq 0$ . Here,

$$d_n = \left[ \prod_{\substack{m=0, \\ m \neq n}}^{\infty} (1 - \lambda_m/\lambda_n) \right]^{-1},$$

and  $\lambda_n$  are the eigenvalues of the integral equation whose kernel is the correlation function of the complex envelope of the random scattered-radiation field:

$$\int_{-T}^T E\langle A_{\text{scat}}(t_1) A_{\text{scat}}^*(t_2) \rangle \theta_m(t_1) dt_1 = \lambda_m \theta_m(t_2), \quad (5)$$

where  $T = L/v_{\text{gr}}$  ( $2T$  is the probe pulse duration);  $v_{\text{gr}}$  is the group velocity of the radiation in the fibre;  $A_{\text{scat}}(t)$  is the complex envelope of the random scattered-radiation field; and  $\theta_m(t)$  are the eigenfunctions of the integral equation. The correlation function of the random field of scattered quasi-monochromatic radiation from a semiconductor laser can be found based on the concept of phase noise, a cause of semiconductor laser line broadening [8, 16, 17]:

$$E\langle A_{\text{scat}}(t) A_{\text{scat}}^*(t + \tau) \rangle = \frac{v_{\text{gr}}^2}{4} \rho_0 I_0 \exp\left(-\frac{|\tau|}{\tau_{\text{coh}}}\right), \quad 0 \leq t \leq 2T, \quad (6)$$

where  $\tau = t_1 - t_2$  is the difference between arbitrary instants of scattering ( $0 \leq \tau \leq 2T$ );  $\tau_{\text{coh}}$  is the coherence time of the laser radiation;  $\rho$  is the spatial correlation coefficient for the complex scattering coefficient of the fibre; and  $I_0$  is the intensity coupled into the fibre.

The shape of the scattered quasi-monochromatic radiation intensity distribution (4) depends on the relationship between the coherence time and the integration time  $2T$  (probe pulse duration) in Eqn (5). Figure 1a shows function (4) normalised to the mean over the ensemble of fibre sections for  $T$  varied from 10 to 200 ns and a constant  $\tau_{\text{coh}}$  of 40 ns. Also shown in Fig. 1a are a nearly exponential distribution for  $\tau_{\text{coh}} \gg 2T$  (monochromatic radiation) and a nearly Gaussian distribution for  $\tau_{\text{coh}} \ll 2T$  (very broad spectrum).

Thus, as the ratio of the coherence time to the probe pulse duration increases, distribution (4) changes from nearly Gaussian to nearly exponential. This means that an observed time-averaged reflectogram depends on the underlying statistical distribution. It is worth noting that, according to the

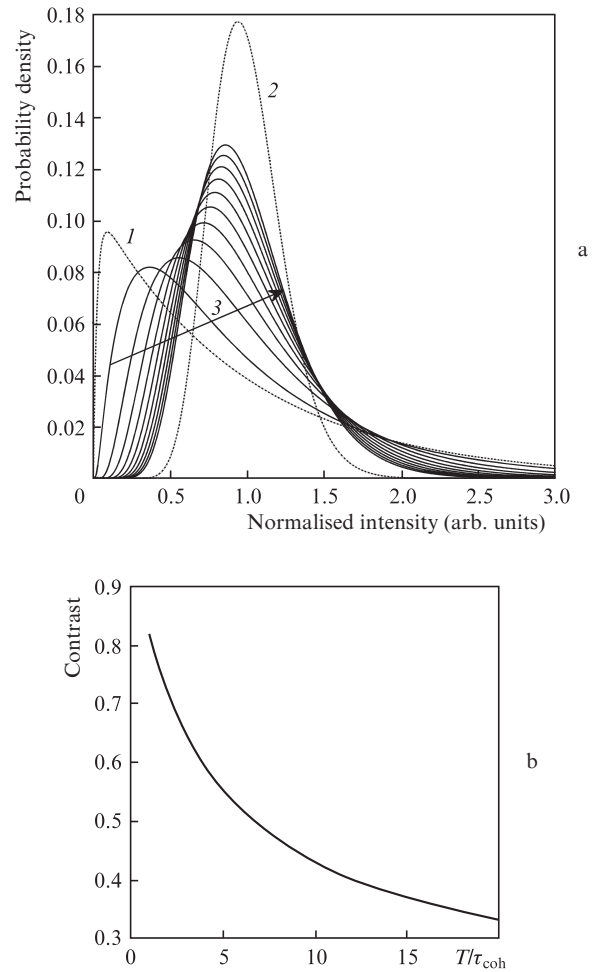


**Figure 1.** (a) Probability distribution densities obtained by solving Eqn (5) and normalised to the mean: (1) limiting case of a nearly exponential distribution approaching (1) for  $T/\tau_{\text{coh}} \ll 1$ , (2) limiting case of a nearly Gaussian distribution for  $T/\tau_{\text{coh}} \gg 1$ , (3) variation in distribution density with increasing  $T/\tau_{\text{coh}}$  (arrow). (b) Theoretical contrast of coherent reflectograms as a function of  $T/\tau_{\text{coh}}$ .

convolution theorem, the coherence time of pulsed radiation cannot exceed the pulse duration. The spectrum of a narrow-band optical signal broadens in response to external pulse modulation. The mean of the resultant random distribution is

$$E\langle I \rangle = \int_0^\infty p_I dI = \sum_{n=0}^\infty d_n \lambda_n, \quad (7)$$

and its variance is

$$\sigma_I^2 = E\langle I^2 \rangle - (E\langle I \rangle)^2 = \sum_{n=0}^\infty 2d_n \lambda_n^2 - \left( \sum_{n=0}^\infty 2d_n \lambda_n \right)^2. \quad (8)$$

The contrast of the resultant reflectogram is then given by

$$C = \frac{\sigma_I}{E\langle I \rangle} = \frac{\left[ \sum_{n=0}^\infty 2d_n \lambda_n^2 - \left( \sum_{n=0}^\infty d_n \lambda_n \right)^2 \right]^{1/2}}{\sum_{n=0}^\infty d_n \lambda_n}. \quad (9)$$

It is fully defined by the set of eigenvalues of Eqn (5) and generally cannot be represented by an analytical expression. Figure 1b shows contrast as a function of  $T/\tau_{\text{coh}}$ . The contrast is seen to monotonically decrease, with the maximum value,  $C = 1$ , corresponding to monochromatic radiation. A reduction in contrast can also be traced in the graph of the distribution function (4) (Fig. 1a): with increasing  $T/\tau_{\text{coh}}$ , the distribution function normalised to the mean narrows down, which corresponds to a reduction in variance. It is worth pointing out that, with increasing pulse duration, the scattered intensity increases because of the rise in the energy delivered to the fibre.

Based on the above analysis, we think that, when a fibre section is employed as a sensing element of a coherent reflectometer, the contrast of reflectograms can be used to quantify its sensitivity to external influences. Since the intensity distribution at each point of a reflectogram is described by function (4), we see that the lower the contrast in the reflectogram, the smaller is the deviation of the intensity at each point from its mean in response to an external influence on the fibre. Thus, the highest sensitivity would be expected for a reflectogram having the highest contrast, i.e., a nearly exponential intensity distribution function. This assumption of course requires experimental verification.

### 3. Experimental

The experimental setup used to study the statistics of the backscatter intensity is shown in Fig. 2. The 1550-nm cw radiation from a distributed-feedback (DFB) semiconductor laser is amplified by an erbium-doped fibre amplifier (EDFA) to 25 dBm. Next, the beam is modulated by 100- $\mu$ s rectangular

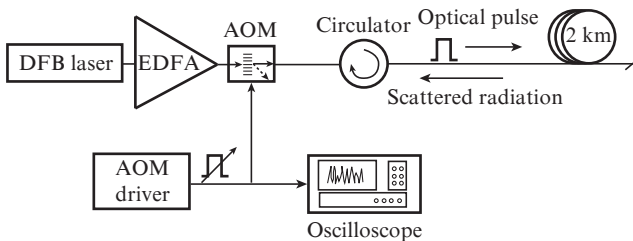


**Figure 2.** Experimental setup used to study the statistics of coherent scattering.

pulses using an acousto-optic modulator (AOM). The pulse duration can be varied from 100 to 500 ns. After the modulator, optical pulses are sent to a 2-km length of SMF-28 fibre through a nonreciprocal element (circulator).

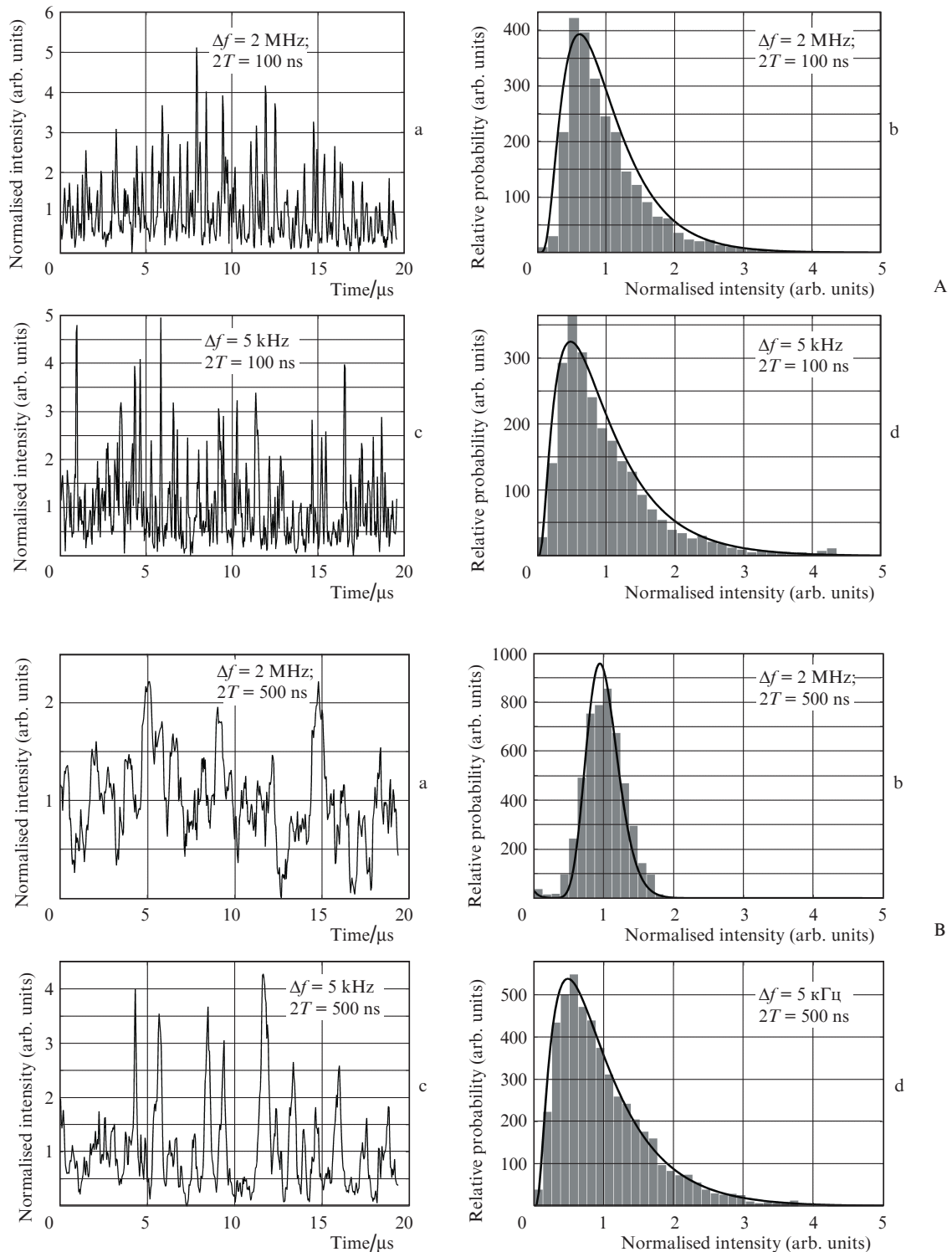
The backscattered light is detected by a 50-MHz photodetector, whose output is coupled to the input of a digital oscilloscope. To exclude the photodetector noise and the spectral noise of the coherently scattered signal in a band twice as broad as that of the pulsed optical signal [11], the oscilloscope took the average over 50 reflectograms. We used two lasers: a standard telecom laser with an emission bandwidth of 2 MHz (which corresponds to a coherence time  $\tau_{\text{coh}} = 160$  ns in continuous mode) and a narrow-band laser with an emission bandwidth of 5 kHz ( $\tau_{\text{coh}} = 64$   $\mu$ s). To find the statistical distribution of the time-averaged scattered intensity, we constructed a histogram of the intensity distribution over an ensemble of independent fibre sections.

Figure 3 shows reflectograms of a 2-km length of fibre for the two lasers at probe pulse durations of 100 and 500 ns. Also shown in Fig. 3 are the corresponding histograms of the scattered intensity distribution over an ensemble of fibre sections and theoretical distribution functions for a particular ratio of the coherence time to the pulse duration. Note good agreement between the calculation results and experimental data.

At a probe pulse duration of 100 ns, which roughly corresponds to the coherence time of the former laser, the reflectograms and scattered intensity distribution functions for the two lasers are identical, and the two distributions have a well-defined exponential portion (Fig. 3A, panels b, d). As the pulse duration increases to 500 ns (with an increase in the extent of the scattering region), the ratio of the pulse duration to the coherence time increases for the 2 MHz bandwidth laser and remains unchanged at about unity for the 5 kHz bandwidth laser. Accordingly, the scattered intensity distribution function approaches a Gaussian for the former laser (Fig. 3B, panel b) and remains unchanged for the latter (Fig. 3B, panel d). The contrast of the reflectograms obtained with the former laser decreases, in accordance with the graph in Fig. 1b, whereas that for the latter laser remains unchanged.

That the ratio of the coherence time to the pulse duration remains unchanged in the case of the 5 kHz bandwidth laser can be qualitatively interpreted as follows: When a narrow-band cw laser radiation is modulated by a signal with a bandwidth that far exceeds the emission bandwidth of the laser, the bandwidth of the resultant modulated signal will be roughly equal to that of the modulating signal. Accordingly, when the laser pulse duration is increased from 100 to 500 ns, the coherence time of the modulated signal will be roughly equal to the modulating pulse duration. Clearly, this is only valid at modulating pulse durations much shorter than the coherence time of the narrow-band laser ( $\tau_{\text{coh}} = 64$   $\mu$ s).

In addition, increasing the probe pulse duration leads to smoothing of the reflectogram. This is because, at a longer pulse duration, each scattering event involves more centres, i.e. a larger number of random phasors. Backscattering occurs continuously as the pulse propagates through the fibre, but at the sampling rate of the oscilloscope used (25 MHz) the backscatter signal is recorded at discrete points in time. At longer pulse durations, the photodetector collects radiation at these points in time from a longer section of the fibre, which includes the section the radiation from which was recorded at the preceding point of data collection. This leads to a smoother shape of the reflectogram.



**Figure 3.** Reflectograms of a 2-km length of fibre and the corresponding histograms of the scattered intensity distribution: pulse duration of (A) 100 and (B) 500 ns; (a, b) low-coherence laser (emission bandwidth  $\Delta f = 2$  MHz, (c, d) high-coherence laser ( $\Delta f = 5$  kHz). The solid lines show calculated probability densities.

Figure 4 shows coherent reflectograms of scattered radiation (normalised to the mean) for the two lasers at probe pulse durations from 100 to 500 ns. Also shown are the corresponding normalised intensity distribution functions. With increasing pulse duration, the variance of the scattered intensity distribution for the shorter coherence time laser decreases and the distribution approaches a Gaussian one (Fig. 3B, panels a, b), whereas the distribution function obtained with the

high-coherence laser remains unchanged and has a well-defined exponential portion (Fig. 3B, panels c, d). This behaviour of the coherent reflectograms is in excellent agreement with theoretical predictions.

It is worth noting that scattering may be accompanied by a reduction in the degree of coherence of the light. Possible reasons for this include depolarisation of the laser radiation at long pulse durations (400 and 500 ns) and nonlinear effects.

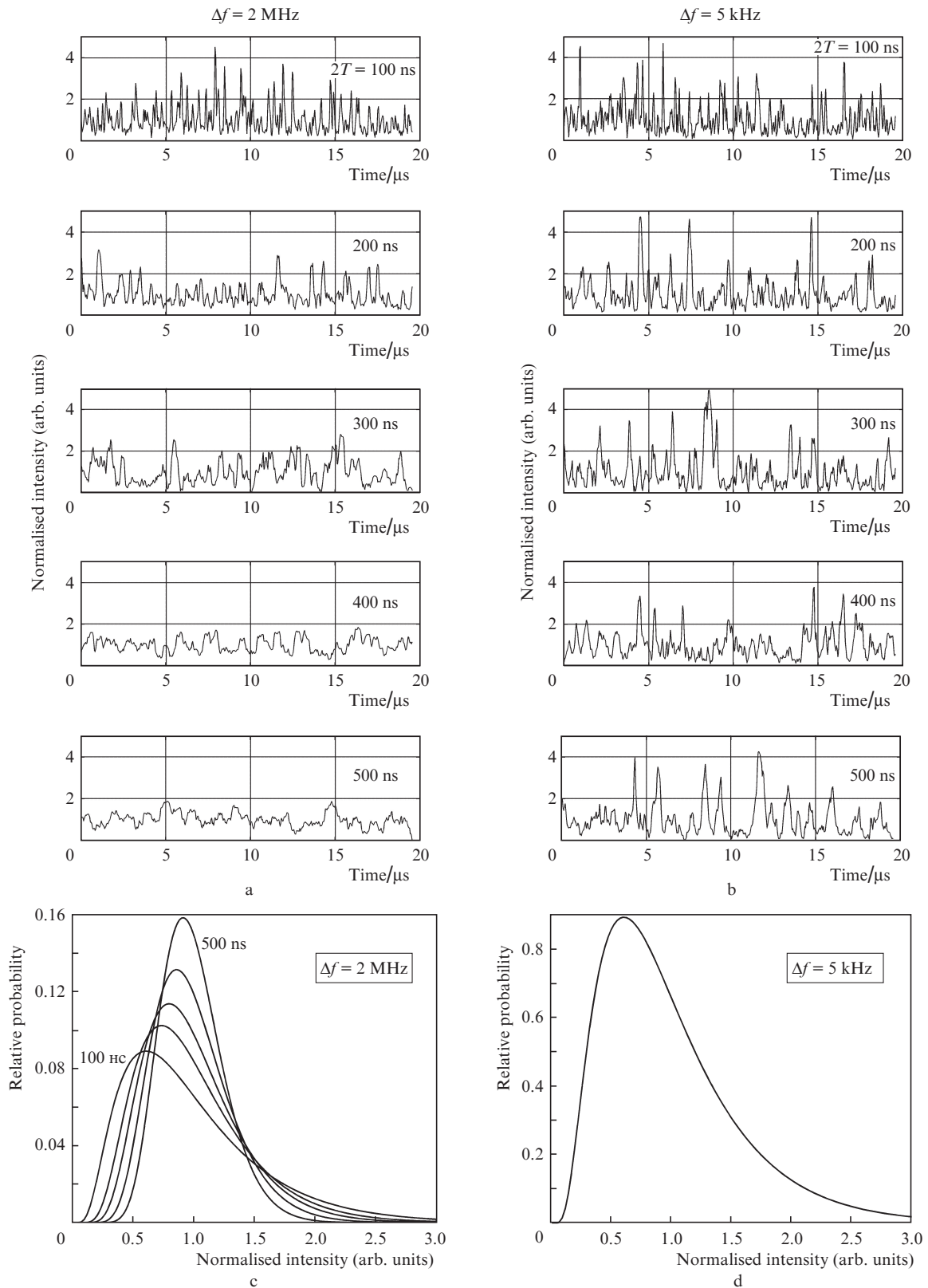


**Figure 4.** Reflectograms of a 2-km length of fibre at probe pulse durations from 100 to 500 ns for the (a) low-coherence and (b) high-coherence lasers and measured intensity distribution functions of the (c) low-coherence and (d) high-coherence lasers at pulse durations from 100 to 500 ns.

These cause the scattered intensity distribution over an ensemble of independent fibre sections to more rapidly approach a Gaussian one.

For a coherent reflectometer, an exponential scattered intensity distribution is preferable: it ensures a higher contrast of reflectograms and, probably, higher sensitivity to external influences.



## 4. Conclusions

Our results lead us to conclude that an exponential distribution of the time-averaged quasi-monochromatic radiation intensity, high contrast of reflectograms, and possibly a higher sensitivity level can be achieved using both a standard telecom semiconductor laser with a 2-MHz bandwidth and a high-coherence laser with a 5-kHz bandwidth at probe pulse durations of 100 ns or shorter. At a probe pulse duration of 500 ns, the coherence time of the former laser is insufficient for obtaining high contrast of reflectograms, whereas with the high-coherence laser the contrast remains at the maximum level. Therefore, a standard telecom DFB semiconductor laser with a 2-MHz bandwidth is suitable for a high spatial resolution (5–10 m) reflectometer. At the same time, if a fibre for a distributed sensor should have a wider sensitivity range (50–100 m or more), the highest sensitivity to external influences in each fibre section can only be achieved with a high-coherence laser.

## References

1. Mamedov A.M., Potapov V.T., Shatalin S.V., Juškaitis R. *Opt. Lett.*, **19** (3), 225 (1994).
2. Gorshkov B.G., Paramonov V.M., Kurkov A.S., Kulakov A.T., Zazirnyi M.V. *Kvantovaya Elektron.*, **36**, 963 (2006) [*Quantum Electron.*, **36**, 963 (2006)].
3. Juarez J.C., Maier E.W., Choi K.N., Taylor H.F. *J. Lightwave Technol.*, **23** (6), 2081 (2005).
4. Nesterov E.T., Treshchikov V.N., Ozerov A.Zh., Sleptsov M.A., Kamynin V.A., Nanii O.E., Sus'yan A.A. *Pis'ma Zh. Tekh. Fiz.*, **37** (9), 55 (2011).
5. Nesterov E.T., Sleptsov M.A., Treshchikov V.N., Nanii O.E., Sus'yan A.A. *Telekommun. Transp.* (8), 51 (2010).
6. Yuelan Lu, Tao Zhu, Liang Chen, Xiaoyi Bao. *J. Lightwave Technol.*, **28** (22), 3243 (2010).
7. Healey P. *Electron. Lett.*, **21** (6), 226 (1985).
8. Alekseev A.E., Tezadov Ya.A., Potapov V.T. *Radiotekh. Elektron.*, **56** (12), 1522 (2011).
9. Hartog A.H., Gold M.P. *J. Lightwave Technol.*, **LT-2**, 76 (1984).
10. Born M., Wolf E. *Principles of Optics* (Oxford: Pergamon, 1969; Moscow: Nauka, 1973).
11. Gysel P., Staubli R.K. *J. Lightwave Technol.*, **8** (4), 561 (1990).
12. Staubli R.K., Gysel P. *IEEE Trans. Commun.*, **40** (6), 1091 (1992).
13. Tosoni O., Aksenov S.B., Podivilov E.V., Babin S.A. *Kvantovaya Elektron.*, **40** (10), 887 (2010) [*Quantum Electron.*, **40** (10), 887 (2010)].
14. Goodman J.W. *Statistical Optics* (New York: Wiley-Interscience, 1985; Moscow: Mir, 1988).
15. Goodman J. W. *Statistical properties of laser speckle patterns in Laser Speckle and Related Phenomena*. Ed. by J.C. Dainty (Berlin: Springer-Verlag, 1975).
16. Henry C.H. *J. Lightwave Technol.*, **LT-4**, 298 (1986).
17. Moslehi B. *J. Lightwave Technol.*, **4** (9), 1334 (1986).